Research Article | Vol. 11, No. 11 / 1 Nov 2021 / Optical Materials Express 3854
Optical Materials EXPRESS

The visible and near-infrared optical absorption coefficient spectrum of Parylene C measured by transmitting light through thin films in liquid filled cuvettes

JAMES A. GUGGENHEIM,[1,2,*] YUANYUAN LYU,[1] DYLAN M. MARQUES,[1] EDWARD Z. ZHANG,[1,3] AND PAUL C. BEARD[1,3]

[1]Department of Medical Physics and Biomedical Engineering, University College London, Gower Street, London, WC1E 6BT, UK
[2]Current address: Institute of Cardiovascular Sciences, University of Birmingham, Edgbaston, Birmingham, B15 2TT, UK
[3]Wellcome/EPSRC Centre for Surgical and Interventional Sciences (WEISS), University College London, Gower Street, London, WC1E 6BT, UK
[*]j.guggenheim@ucl.ac.uk

Abstract: Parylene C (PPXC) is a polymer deposited from the gas phase to form optically clear thin films used in devices including waveguides and sensors. The performance of these devices depends on the visible and near infrared absorption coefficient of PPXC. However, the absorption coefficient is difficult to measure. This is because PPXC films are typically too thin to exhibit detectable absorption in conventional transmittance measurements. To address this challenge, a method involving measuring the transmittance of multiple films immersed together in a liquid filled cuvette was devised. This increased the sensitivity to absorption by increasing the path length in PPXC, while also minimizing reflections and surface losses. Using 200-500 μm thick films, this method was applied to measure the absorption coefficient of PPXC at wavelengths in the range 330-3300 nm. The coefficient was found to vary spectrally by more than two orders of magnitude from 0.025 mm^{-1} at 1562 nm to 7.7 mm^{-1} at 3262 nm. These absorption measurements could aid the design of PPXC based sensors and waveguides. The method could be useful for measuring the absorption coefficient of other thin, low-loss materials, particularly those for which it is challenging to obtain thick samples such as other polymers deposited from the gas phase in a similar manner to PPXC.

1. Introduction

Polyparachloroxylylene (PPXC) [1], also known as Parylene C, is a polymer that usually exists in the form of thin (sub-100 μm thick) films fabricated via chemical vapor deposition. These films are commonly used to provide protective barrier coatings for implanted medical devices [2], optoelectronics [3] and other components, affording properties such as biocompatibility and moisture resistance [2]. In optics, PPXC films are also used to provide a light transmitting layer in devices such as waveguides [4–8] and resonant optical sensors [9–12]. The applications of PPXC based optical devices are diverse, spanning fields including neurophotonics and biomedical imaging. For example, PPXC waveguides have been proposed for transmitting light into the brain for optogenetic stimulation and neuroimaging at a range of visible wavelengths [6,8]. Elsewhere, PPXC based sensors have been developed for use as temperature probes [12] and ultrasound detectors used in photoacoustic imaging [9–11].

#427952 https://doi.org/10.1364/OME.427952
Journal © 2021 Received 11 May 2021; revised 2 Sep 2021; accepted 2 Sep 2021; published 21 Oct 2021

Optical Materials EXPRESS

In the above applications, the role of PPXC is to transmit light from one place to another and the transmission efficiency affects the device performance. For example, in PPXC based optogenetic waveguides [6], sufficient light must be transmitted through the waveguide to elicit neuronal activation [13]. Likewise, in optically resonant ultrasound sensors made from PPXC [9–11], light must be transmitted efficiently, back-and-forth through a PPXC layer to provide high sensitivity. As the transmissivity of PPXC underpins the performance of these devices, there is a need to quantify light absorption in PPXC.

PPXC films typically appear visually transparent [3]. However, this is not because the films are non absorbing but because they have a low thickness. The combination of this low thickness and a sufficiently low absorption coefficient means almost no light is lost when transmitted once through a film at normal incidence. In the above mentioned devices however, light must commonly travel distances orders of magnitude larger than the PPXC film thickness. In waveguides, this can occur because the light travels parallel to the film plane [4–7]. In optically-resonant sensors, it happens because the light makes many (hundreds or even thousands of) round trips inside the PPXC layer [9–12]. In both cases, the path lengths in PPXC can readily exceed several cm, over which distances optical losses accumulate to the extent that they impact upon the device performance [4,5,7]. Predicting the limits of the performance of these devices, the maximum transmissivity of waveguides or sensitivity of sensors for example, therefore requires accurately quantifying the absorption coefficient of PPXC. Due to the range of different wavelengths used in PPXC based optical devices (e.g. 450-680 nm [4–7] and 1440-1640 nm [9–12,14]), this coefficient is of interest at a broad range of wavelengths throughout the visible and near infrared spectrum.

PPXC absorption has been studied previously. However, previous measurements do not provide an accurate visible and near infrared PPXC absorption coefficient spectrum. In one study, Bera et al. [15] studied the relative spectral characteristics of PPXC absorption using measurements of the total transmittance of a 46 µm thick PPXC film at wavelengths of 280-500 nm, before and after irradiating the film using UV light to study its subsequent discoloration [15]. Elsewhere, Jeong et al. [3] also reported a PPXC transmittance spectrum, spanning the wavelength range 200-1000 nm. Aside from the limited wavelength ranges of these measurements, their main limitation is that they were not corrected for Fresnel reflections, as such they quantify losses that are not specific to absorption. The measurements also suffered limited accuracy due to the low thicknesses of the studied films, particularly at wavelengths where PPXC is highly transparent. For these reasons, it is challenging to estimate the absolute PPXC absorption coefficient from these measurements.

In another study, Xie et al. [8] measured a PPXC absorption coefficient of 0.17 mm^{-1} by transmitting blue LED light through multiple PPXC films with thicknesses in the range 15-100 µm. It is difficult to ascertain the accuracy of this coefficient however, because the custom system was unconventional and not characterized.

Two other studies reported PPXC attenuation coefficients calculated from estimates of the light intensity transmitted along PPXC waveguides [5,6]. In these studies, a camera was used to image the light scattered out of the side wall of the waveguide, and an exponential function was fitted to the out-scattered intensity as a function of distance along the waveguide. Reddy and Chamanzar [5] used this method to estimate the attenuation in a handful of PPXC waveguides using light with a wavelength of 532 nm. Reddy et al. [6] then applied the same method to characterize a larger number of PPXC waveguides at wavelengths of 450 nm, 532 nm, 633 nm and 680 nm. It is difficult to assess the validity of these measurements however. The main reason is the accuracy of the measurement method is unknown and does not appear to have been investigated. In addition, the reported details of the measurement systems were incomplete, the system was not characterized, and none of the measurements were independently verified. Moreover, across the two studies, only one image was shown of the out-scattered light intensity along a waveguide [5], and this had a low signal to noise ratio (SNR), exhibiting variations on the order of 50-100%

Optical Materials EXPRESS

of the measured intensity, with no apparent resemblance to an exponential trend as expected in the data. Finally, absorption was evidently not the only loss mechanism, because some light was scattered out of the waveguide.

Given the uncertain accuracy and limited wavelength range of previous PPXC absorption measurements, there is a need to accurately measure the visible and near infrared absorption coefficient spectrum of PPXC.

The main challenge associated with measuring the absorption coefficient of thin, highly transparent PPXC films is that the absorption related losses are often so low that they simply cannot be detected using conventional transmittance measurements [16–19]. In principle, this could be straightforwardly addressed by using a much thicker film. However, it is challenging to fabricate PPXC films that are thick enough to provide accurate measurements.

To address this challenge, a new method was developed. This method extends the approach of Heitmann [19], who measured the internal transmittance of weakly absorbing glass samples by immersing single samples in liquid-filled cuvettes to reduce the refractive index contrast at the sample interfaces. This minimized reflections and surface scattering, increasing the accuracy of subsequent absorption calculations. In the present study, Heitmann's approach is extended to immersing multiple PPXC films in the same liquid-filled cuvette. As well as minimizing reflections and surface scattering, using multiple films increases the path length in PPXC, thereby increasing the detectability of absorption related losses, without requiring a thicker sample. As another means of increasing the total path length and thus the sensitivity, PPXC films with a high thickness of 200-500 µm were custom fabricated. Measurements involving up to ten of these films enabled transmittance measurements to be made with path lengths of up to 5 mm. Measurements were made in the wavelength range 330-3300 nm.

The remainder of the paper details the method and describes its application to measuring the absorption coefficient of PPXC. Section 2 explains the theoretical basis for the method. Section 3 describes how it was applied to measure the absorption coefficient of PPXC. Section 4 presents the results including the absorption spectrum of PPXC. Sections 5 and 6 provide discussions and conclusions.

2. Theory

From Lambert's law, the absorption coefficient of a homogeneous non-scattering material is:

$$\mu = -\frac{\log \tau}{d}, \tag{1}$$

where τ is the internal transmittance (the transmittance excluding losses due to reflections at the entrance and exit surfaces [29]) of the material over a path length d.

Equation (1) allows calculating the absorption coefficient of a thin film material from a measurement of its internal transmittance. In a conventional transmittance measurement, light could be transmitted through a film at normal incidence as shown in Fig. 1(a). Neglecting multiple internal reflections and any scattering due to surface imperfections, the intensity transmitted through the film would be:

$$T_f = \tau_f \, F^2_{air \to film}, \tag{2}$$

where τ_f is the internal transmittance of the film and $F_{air \to film} = F_{film \to air}$ is the interfacial Fresnel transmission coefficient of its surfaces, defined using the Fresnel equation:

$$F_{1 \to 2} = \left(\frac{4 n_1 n_2}{(n_1 + n_2)^2} \right), \tag{3}$$

where n_1 and n_2 are the refractive indices of the media (labelled 1 and 2) on either side of the interface, in this case the film material and air.

Optical Materials EXPRESS

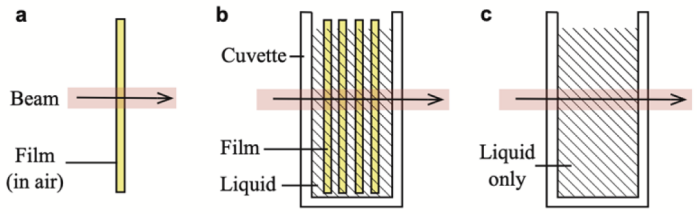

Fig. 1. Schematics showing a beam of light transmitted through (a) a film, free-standing in air, (b) a liquid-filled cuvette containing four films (c) a liquid-filled cuvette without films.

Equation (2) and 3 allow calculating the absorption coefficient of a film from a conventional transmittance measurement. However, if the film is weakly absorbing and thin, this method can provide insufficient sensitivity to absorption. Due to the presence of two closely spaced high-contrast optical interfaces presented by the film surfaces, the method is also susceptible to errors associated with (i) multiple internal reflections, which are not accounted for in Eq. (2) (ii) inaccuracy in the knowledge of the refractive index of the film, which propagates to inaccuracy in the Fresnel coefficients (iii) surface scattering due to film imperfections (iv) deviations from a collimated, normally incident beam.

If, instead, light is transmitted through m films immersed in a liquid filled cuvette as shown in Fig. 1(b) (for $m = 4$), then the light will be absorbed in the liquid, in the cuvette walls, and in the films, and partially reflected at each of the air-cuvette, cuvette-liquid and liquid-film interfaces. Therefore, neglecting multiple internal reflections and scattering due to surface imperfections, the total transmittance can be written as:

$$T_m = \tau_c \tau_f \, e^{-\mu_l (L-D)} \, \mathrm{F}^2_{\mathrm{air}\rightarrow\mathrm{cuvette}} \mathrm{F}^2_{\mathrm{cuvette}\rightarrow\mathrm{liquid}} \mathrm{F}^{\mathrm{m}}_{\mathrm{film}\rightarrow\mathrm{liquid}}, \tag{4}$$

where: τ_c is the total internal transmittance of both of the cuvette walls, defined by the wall thicknesses and the absorption coefficient of the cuvette wall material; $\tau_f = e^{-\mu_f D}$ is the internal transmittance of the film material accumulated across all the films, where D is the total path length in the film material, defined as $D = \sum_{i=1}^{m} d_i$, where d_i is the thickness of each film, and μ_f is the film absorption coefficient; $e^{-\mu_l (L-D)}$ is the internal transmittance of the liquid, where μ_l is the absorption coefficient of the liquid and L is the cuvette path length; and the F terms, defined as in Eq. (3), describe the transmissivities of the different optical interfaces in the sample.

Equation (4) permits calculating the internal transmittance of the film material from a single transmittance measurement, given knowledge of the absorption coefficient of the cuvette wall material and the liquid, and the refractive index and total thicknesses of the liquid, cuvette wall, and film materials. The calculation can be simplified however, its accuracy improved, and the need for knowledge of the cuvette material obviated, by performing a reference measurement. This requires removing the films so the cuvette contains liquid only, as shown in Fig. 1(c). The total transmittance is now:

$$T_0 = \tau_c \, e^{-\mu_l L} \, \mathrm{F}^2_{\mathrm{air}\rightarrow\mathrm{cuvette}} \, \mathrm{F}^2_{\mathrm{cuvette}\rightarrow\mathrm{liquid}}, \tag{5}$$

Dividing Eq. (5) by Eq. (4) yields:

$$\frac{T_0}{T_m} = \frac{e^{-\mu_l D}}{\tau_{\mathrm{f}} \, \mathrm{F}^{\mathrm{m}}_{\mathrm{film}\rightarrow\mathrm{liquid}}}, \tag{6}$$

which, rearranged, provides the following expression for the internal transmittance of the film:

$$\tau_{\mathrm{f}} = \frac{T_m}{\mathrm{T}_0} C, \tag{7}$$

Optical Materials EXPRESS

in which the term

$$C = \frac{e^{-\mu_l D}}{F^{m}_{\text{film}\rightarrow\text{liquid}}} \tag{8}$$

can be considered a correction for measured losses unrelated to film absorption.

Using Eq. (1) and Eq. (7), the absorption coefficient of a film material can be determined from measurements of T_0 and T_m, given knowledge of the absorption coefficient of the liquid, the thickness of the films, and the refractive indices of the liquid and the film material. Compared to estimating the absorption coefficient of a weakly-absorbing thin film material from the transmittance of a single film in air, this has two advantages. Firstly, using multiple films extends the path length in the film material, increasing the sensitivity to absorption. Secondly, immersing the films reduces the refractive index at the film surfaces, reducing the magnitude of reflections and thus the size and impact of (i) higher order reflections (ii) errors in the calculated surface transmissivity (iii) surface scattering. In the limit where the liquid is negligibly absorbing and the indices of the film and liquid are identical, C goes to 1 and the absorption coefficient of the film can be obtained directly from the ratio of the two transmittance measurements.

To summarize, the above constitutes an alternative method for measuring the absorption coefficient of a weakly absorbing thin film material that can, in principle, provide significantly higher accuracy than a conventional transmittance measurement.

3. Methods

3.1. PPXC film preparation

PPXC films were fabricated using a commercial PPXC deposition system (PDS 2010 Labcoater 2, Speciality Coating Systems). To increase the sensitivity of the absorption measurements, the films were fabricated with a relatively high thickness of 200-500 µm as follows. Firstly, a thin PPXC film was grown on a polymethylmethacrylate (PMMA) substrate. This film was peeled from the substrate, then returned to the deposition system, suspended on a hollow frame such that PPXC could then be grown on both sides of the film simultaneously over several further deposition runs. Doing this yielded a PPXC film several cm in diameter with a thickness of 473 µm. This thickness was determined interferometrically by measuring the reflection spectrum of the film in the wavelength range 1440-1640 nm using a system developed to interrogate polymer film interferometers [9]. Due to interference in the film, its reflectivity exhibited a large number of spectral interference minima, the spacings between which were used to estimate the film thickness [14].

From the fabricated PPXC film, ten sub-films of lateral dimensions 9 mm × 40 mm were cut to fit snugly in an optical cuvette. Each of these new films was arbitrarily assigned a partner film, providing five labelled film pairs.

The above process was repeated once using fewer coating runs to produce five 219 µm films.

All the films were visually clear. However, some had surface defects resembling scratches, possibly an imprint of imperfections on the substrates.

3.2. Transmittance measurements

To measure the absorption coefficient of PPXC and the host liquid used in the cuvettes, we measured the wavelength-resolved transmittance of liquid-filled cuvettes with and without added PPXC films (Fig. 1). We also measured the transmittance of single PPXC films in air.

3.2.1. Spectrophotometer

A double-beam spectrophotometer (Lambda 750S, Perkin Elmer) was used to make transmittance measurements. In this spectrophotometer, broadband light is generated by a deuterium (UV) and a tungsten-halogen (VIS-NIR) lamp and spectrally filtered by a monochromator with a

Optical Materials EXPRESS

programmable slit width and central wavelength in the range 190-3300 nm. After filtering, the light is collimated and apertured to provide a beam with a rectangular spatial profile. This beam passes through a sample chamber in which it is weakly-focused on a pre-aligned cuvette holder. The beam is then steered into a detection module in which its intensity is measured. Two detection modules were used. One was a "standard" module in which light was detected by a photomultiplier tube (PMT; if $\lambda < 860$ nm) or a lead-sulphide detector (if $\lambda > 860$ nm). The other was a "sphere" module, in which light was detected by either a PMT (if $\lambda < 860$ nm) or an InGaAs detector (if $\lambda > 860$ nm), both housed in an integrating sphere, allowing the detection of light scattered through a sample into multiple directions.

The spectrophotometer has two optical paths, a "sample arm" and a "reference arm". In each of these arms, the beam travels a similar distance and encounters a similar sample chamber. The reference arm performs two roles. Firstly, it acts to reduce errors due to temporal changes in the sensitivity of the spectrophotometer, e.g., due to drifts in the lamp intensity. To minimize such errors, the spectrophotometer records the ratio of the light intensities measured near-simultaneously in the sample and reference arms. Secondly, to increase the SNR of its light intensity measurements, the spectrophotometer automatically tunes its sensitivity (detector gain and monochromator slit width) to match the light intensity available in the reference arm. In these conditions, the spectrophotometer can be optimized to detect the amount of light transmitted through the sample in the sample arm with high SNR if an object of similar transmittance is placed in the reference arm. When measuring the transmittance of a liquid-filled cuvette with added films for example, a suitable reference object could be a similar cuvette without added films. In the present study however, it was found that using the reference arm in this way had little impact on the uncertainty in our PPXC transmittance and absorption measurements. This was because this uncertainty was limited by systematic factors (e.g., cuvette surface cleanliness and uncertainty on the corrections), rather than the error on individually measured transmitted intensities. For this reason, reference cuvettes were used only in some and not all of the measurements, as indicated below.

3.2.2. Cuvettes

The optical cuvettes used in this study were made of fused silica (QX, Hellma Optics) or glass (OS, Hellma Optics), and had path lengths in the range 2-20 mm. The cuvette materials had known spectrally-resolved refractive indices, supplied by the manufacturer. Cuvettes were cleaned using isopropanol before each transmittance measurement.

3.2.3. Measurements

For a selected wavelength, the spectrophotometer measures the ratio of the transmitted light intensity measured in its sample arm, S, and in its reference arm, R. i.e., the measurement is:

$$M_{sample} = \frac{S}{R} = \frac{P_{sa}T_s + O}{P_{ra}T_r + O}, \tag{9}$$

where: P_{sa} and P_{ra} are the sample-free transmittances of the sample and reference arms; T_s and T_r are the transmittances of objects positioned in the arms (the sample and reference materials); and O is a detector offset. To eliminate the unknowns in Eq. (9) and obtain the transmittance of the sample, T_s, two further measurements are needed in addition to M_{sample}. In the first, $M_{open} = (P_{sa} + O)/R$, the sample is removed such that T_s becomes 100%. In the second, $M_{dark} = O/R$, the sample is replaced by a fully opaque object such that T_s becomes zero. Note, if a reference material is used in the reference arm, this must be identical in all three measurements.

Optical Materials EXPRESS

T_s can then be computed as:

$$T_s = \frac{M_{sample} - M_{dark}}{M_{open} - M_{dark}} \tag{10}$$

We pre-programmed the spectrophotometer to make a series of these measurements at different wavelengths in sequence with a chosen minimum and maximum wavelength, wavelength step, and spectral slit width. Samples were positioned either in the fixed, pre-aligned cuvette holder in the sample arm (in the case of 5-10 mm cuvettes), or directly in front of this holder (in the case of free-standing films or larger cuvettes). All measurements were recorded to a computer for offline processing. When measuring M_{dark}, the sample arm was blocked with an opaque aluminium block.

4. Results

4.1. Host liquid characterization

Measuring absorption in PPXC films in liquid filled cuvettes required selecting a suitable host liquid in which to immerse the films. The principal requirement for the liquid was that its refractive index was known and well matched to that of PPXC in order to minimize (i) surface scattering due to any film imperfections and (ii) the Fresnel reflection coefficient at the film surface and thus reduce the magnitude of the errors associated with its calculation. A further requirement was that the liquid should be weakly absorbing. Based on these requirements, a commercial refractive index matching liquid (50350, Cargille Laboratories) was chosen to act as the host liquid. This liquid had a well-known refractive index, was sufficiently well matched to PPXC, and was sufficiently transparent (at many wavelengths) as discussed further below.

4.1.1. Refractive index

Quantifying the refractive index mismatch between the host liquid and PPXC required obtaining the index of both materials over the wavelength range of interest. The indices of both materials were also needed to calculate the total interfacial transmittances of samples and the liquid absorption coefficient, both of which were required for calculating the absorption coefficient of PPXC films.

Based on a literature review, it was found that the refractive index of PPXC in the plane of the film (PPXC is birefringent) is represented well by the Cauchy equation:

$$n_{PPXC} = 1.618 + (1.17 \times 10^{-2})\,\lambda^{-2}, \tag{11}$$

in which λ is the wavelength in micrometers. This equation is based on refractive index measurements at wavelengths in the range 400-1000 nm [20] and provides values consistent with other reported measurements in this wavelength range [1,3,5,7]. For the refractive index of the liquid, the manufacturer provided a Cauchy equation based on measurements in the wavelength range 225-1550 nm:

$$n_{liquid} = 1.4469 + (3.99 \times 10^{-3})\,\lambda^{-2} + (3.76 \times 10^{-5})\,\lambda^{-4}. \tag{12}$$

At wavelengths outside these ranges, refractive index data could not be found for either material so it was assumed that Eq. (11) and Eq. (12) remained valid for all other wavelengths in the 330-3300 nm range of interest. Using these equations, the refractive indices of PPXC and the liquid were calculated and plotted in Fig. 2 (left axis). Over the plotted wavelength range, the index of PPXC is in the range 1.62-1.72, while that of the liquid is in the range 1.44-1.49. The indices of the materials are therefore matched to within about 0.2. The Fresnel reflection coefficients for a PPXC-air interface and a PPXC-liquid interface were calculated and are also plotted in Fig. 2 (right axis). The coefficients for a PPXC-liquid interface are well below 1% and

Optical Materials EXPRESS

more than an order of magnitude lower than those for a PPXC-air interface. Consequently, low errors are expected when calculating the interfacial transmittances of PPXC films in this liquid and any residual surface scattering due to film imperfections is expected to be minimal.

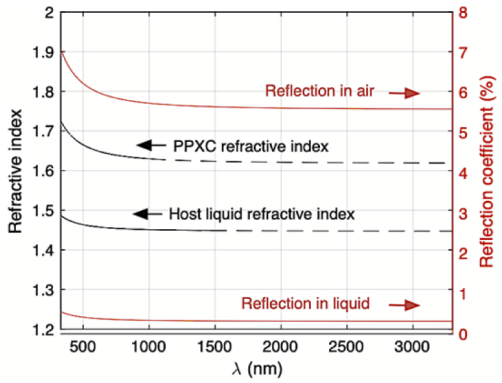

Fig. 2. Refractive index of PPXC [20] (in the plane of the film) and host liquid (left axis, colored black), and Fresnel reflection coefficients of PPXC films in air and liquid (right axis, colored red). In the refractive index plots, solid lines indicate values within the wavelength ranges of the measurements from which the refractive index data were derived, while dashed lines indicate values outside these ranges.

4.1.2. Absorption coefficient

To measure the absorption coefficient of the liquid, we measured the transmittance of a cuvette filled with the liquid. To account for absorption in the cuvette walls, we also measured the transmittance of the same cuvette when empty. The internal transmittance of the liquid was obtained by computing the ratio of the liquid-filled and empty cuvette transmittances, after correcting for reflections. The absorption coefficient was calculated using Eq. (1).

To validate the method, we measured the absorption coefficient spectrum of water. Measurements were made using 2, 10, and 20 mm cuvettes and combined to produce a single absorption spectrum. The calculated spectrum is plotted in Fig. 3 along with the known absorption spectrum of water [21]. The data are in close agreement suggesting the method is valid. The same procedure was then applied to measure the absorption coefficient spectrum of the host liquid, which is also plotted in Fig. 3. In general terms, the absorption coefficient of the liquid increases with increasing wavelength, spanning a large range of values, from 0.001 mm^{-1} or lower to about 3 mm^{-1}. The spectrum also exhibits a number of local peaks such as at 1720nm as marked on the plot (and referred to below in the following section). Absorption coefficients were also calculated using transmittance data provided by the liquid supplier at certain discrete wavelengths. These coefficients are in good agreement with the other measurements.

4.2. PPXC absorption measurements

To obtain a first indication of the PPXC absorption spectrum, conventional transmittance measurements were performed using single PPXC films in air. Next, the method described in section 2 was applied to measure the absorption coefficient of PPXC using four PPXC films immersed in liquid. Finally, to provide additional confidence in the results, it was decided to repeat the measurements made in liquid using different numbers of films, different total film thicknesses, different cuvettes, and different detectors to see whether the results agreed.

Optical Materials EXPRESS

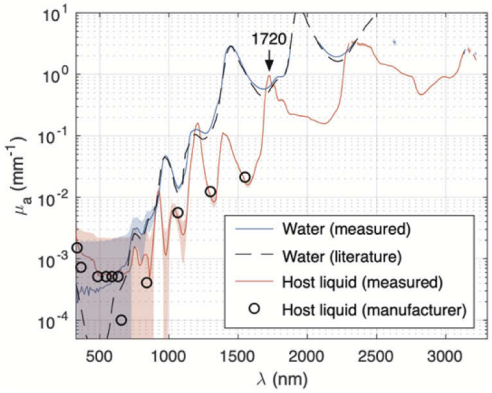

Fig. 3. Absorption coefficient spectra of the host liquid and deionized water. Measured absorption values are plotted along with liquid values calculated from the supplier's transmittance data and water measurements from literature [21]. The shaded regions show uncertainties ($\pm 1\sigma$) based on the measurement error and the uncertainties associated with the reflection corrections.

4.2.1. PPXC absorption measurements using films in air and in liquid

The transmittances of individual 473 µm thick PPXC films were measured in air. The internal transmittance was obtained using Eq. (2), after estimating the Fresnel transmission coefficients of the film surfaces using Eq. (3). The absorption coefficient of the film was then calculated using Eq. (1). The measurements were made using a subset of the available PPXC films and repeated several times. No reference material was used in the reference arm of the spectrophotometer.

Measurements were then made using 473 µm thick films in liquid. The transmittance of a liquid-filled cuvette was measured with and without four added films. The internal transmittance and absorption coefficient of the films were calculated as described in section 2. These measurements were made using all ten possible combinations of two of the five available PPXC film pairs and repeated, yielding 20 independent measurements. A similar liquid-filled cuvette (without films) was used as a reference material in the reference arm of the spectrophotometer.

The internal transmittance and absorption coefficient spectra for PPXC films measured in air and in liquid are plotted in Fig. 4. The transmittance measurements in air (Fig. 4(a), grey line) show a broadband transmission window spanning almost the full wavelength range of the measurements. Within this window, there are a number of minima, for example at 1144 nm, 1384 nm, 2168 nm, and (several) around 2440 nm. The relative uncertainty is about 3% at most wavelengths, although this is higher at the spectral extremes of the measurements.

As expected from the internal transmittance spectrum, the absorption spectrum measured in air (Fig. 4(b), grey line) reveals a broad window with the highest absorption near the spectral limits of the measurement. The spectrum also contains absorption peaks corresponding to each of the measured transmittance minima. Compared to the uncertainties on the transmittance, the uncertainties on the absorption coefficients are significantly more variable. This is a consequence of the nonlinear propagation of the uncertainty in the transmittance via the logarithm operator in Eq. (1). This means that a given uncertainty in the transmittance maps to a higher uncertainty in the absorption coefficient when the transmittance is higher. Uncertainties in the absorption coefficients are therefore typically higher when the transmittance is high. For instance, in the wavelength range 550-1650 nm, where the transmittance is near 100%, the uncertainty in the absorption coefficient is one to several times the value of the absorption coefficient. By contrast, at wavelengths higher than 2120 nm, where the transmittance is <90%, the uncertainty in the absorption coefficient is lower (in the range 3-33%).

Optical Materials EXPRESS

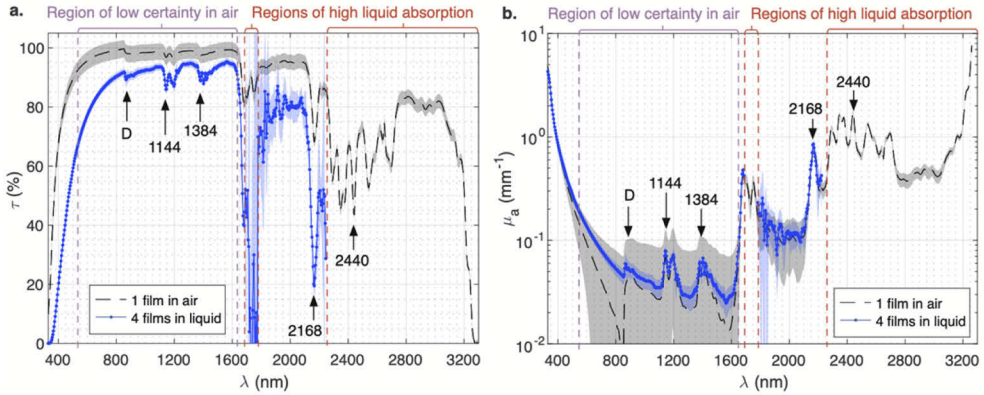

Fig. 4. (a) Internal transmittance and (b) absorption coefficient of single PPXC films in air and four PPXC films in liquid. These data are based on transmittance measurements using 473 μm thick PPXC films, a wavelength step of 4 nm, and a slit width of 1 nm (liquid) or 2 nm (air). The shaded regions show uncertainties ($\pm 1\sigma$) based on the measurement error and the uncertainties associated with the host liquid absorption and interfacial reflection corrections. The arrow marked "D" indicates a known artefact related to the spectrophotometer switching between its two detectors. Other arrows highlight spectral features (in nm), as referred to in the main text. Measurements in liquid were limited to wavelengths <2250 nm because, at longer wavelengths, high absorption in the liquid (Fig. 3) prevented accurate measurements being made.

The internal transmittance of PPXC measured using four films in liquid (Fig. 4(a), blue line) is lower than the transmittance measured using one film in air, as expected due to the larger total thickness of PPXC. At most wavelengths <1670 nm, the uncertainties are typically about 1.5%, i.e., about half those seen in air. These lower uncertainties are likely a consequence of the reduced surface scattering and lower interfacial reflections when the films are in the liquid. At longer wavelengths, the uncertainties are higher and more variable, and higher than those seen in air. For example, they are >30% at wavelengths in the range 1690-1780nm, and in the range 2-20% at 1800-2200 nm. These higher uncertainties are a result of high light absorption in the host liquid (Fig. 3) leading to a lower transmittance through the samples and therefore lower accuracy. In the most extreme cases, prohibitively high liquid absorption led to transmittance being effectively unmeasurable. This occurred both near to 1720nm, where the absorption coefficient of the host liquid peaks locally (Fig. 3), and at wavelengths >2250 nm. To highlight these spectral bands, they are labelled "regions of high liquid absorption" in Fig. 4.

The absorption spectrum calculated from the measurements made in the liquid (Fig. 4(b), blue line) agrees with the spectrum calculated from the measurements made in air. However, the uncertainties are typically significantly lower. For example, at wavelengths below 1670 nm, the uncertainties are in the range 1-30% and about an order of magnitude lower than those obtained in air. This is mainly due to the nonlinear mapping of transmittance to absorption described above. In other words, decreasing the transmittance by extending the path length in PPXC by using multiple films reduced the uncertainty on the absorption coefficient. To a lesser degree, the lower uncertainties are also a consequence of the reduced surface scattering and lower Fresnel reflection coefficients that arise when the films are in the liquid. The exception is at wavelengths where the host liquid absorption was prohibitively high. For these wavelengths, absorption data is not plotted because it was obviously erroneous. Fortunately, in these spectral bands (marked "regions of high liquid absorption" in Fig. 4), the absorption coefficient of PPXC was found to be sufficiently high that the measurements in air were highly accurate. Thus, between them, the air

Optical Materials EXPRESS

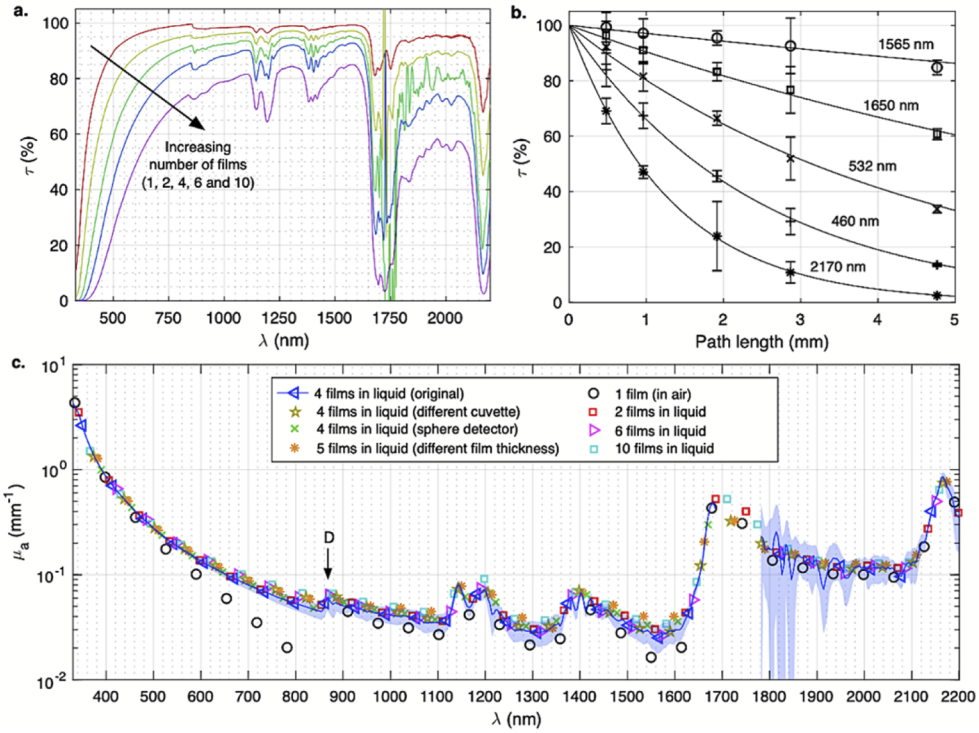

Fig. 5. PPXC internal transmittance and absorption coefficient spectra obtained using different numbers of films, different cuvettes and different detectors. (a) Internal transmittance measured using 1, 2, 4, 6 and 10 PPXC films. For 1 film and 4 films, the data is the same as the data plotted in Fig. 4. For 2, 6 and 10 films, measurements were made in liquid. (b) Internal transmittance as a function of path length in PPXC at selected wavelengths, sampled from the transmittance plots in (a). (c) PPXC absorption coefficient spectra obtained using different numbers of films, different cuvettes, films of different thickness, and two different detectors (one standard detector and one integrating sphere based detector). In (a) and (c), the wavelength range is limited to <2200 nm because measurements in liquid were inaccurate due to high liquid absorption at longer wavelengths (Fig. 3). To de-clutter the graph, uncertainties are omitted except in the original 4 film data and datasets were down-sampled to limit the number of plotted points. "D" marks the detector step artefact described in the caption of Fig. 4.

and liquid based methods provided accurate absorption measurements across the majority of the studied spectral range (see section 4.2.3).

4.2.2. Measurements using multiple film thicknesses, different numbers of films, different liquid path lengths, different cuvette materials, and different detectors

To provide additional confidence in the measured PPXC absorption coefficients, it was decided to repeat the measurements using different numbers of films, different total film thicknesses, a different cuvette made of a different material and with a shorter path length, and different detectors to see if the results agreed.

First, the PPXC measurements performed in liquid (Fig. 4) were repeated using two, six and ten films. The resulting transmittance spectra are plotted in Fig. 5(a), along with the original one and four film data. As expected, the transmittance decreased as the number of films increased, due to the increasing path length in PPXC. To verify that this reducing transmittance followed

Optical Materials EXPRESS

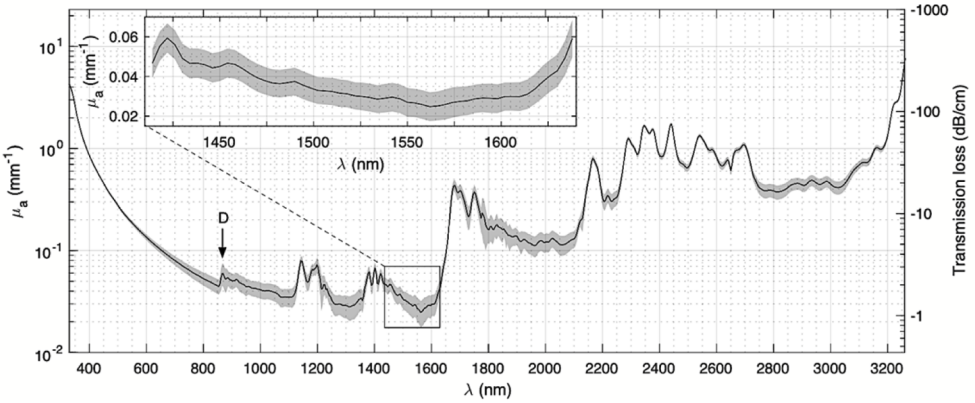

Fig. 6. PPXC absorption spectrum obtained by combining multiple datasets to provide high accuracy over the whole plotted wavelength range. The arrow labelled "D" indicates the detector step. The inset shows a zoomed in version of the plot of the absorption coefficient in the wavelength range 1410-1640 nm. Light with a wavelength in this range is commonly used in PPXC based optical sensors [9] and in optical telecommunications (note: there is a linear Y axis scale on the inset only). For convenience, the right-hand Y-axis presents the measured absorption as an equivalent transmission loss in units of dB/cm. This is defined as $10 \times \log_{10}(T_{1\mathrm{cm}})$, where $T_{1\mathrm{cm}} = e^{-(\mu_a \times 1\mathrm{cm})}$ and represents the fractional power transmitted over a path length of 1 cm in PPXC. The data underlying this figure is available in Dataset 1 [22].

an exponential decay with increasing path length as expected from Eq. (1), the transmittance was plotted as a function of the path length in PPXC for selected wavelengths in Fig. 5(b), with exponential functions fitted to the data. These provided a good fit and the exponential constants were consistent with the absorption coefficients obtained in the original measurements.

Next, to test the robustness of the measurements to parameters other than the number of films, the measurements in liquid were repeated in other conditions. Firstly, the measurements were repeated using a different cuvette made from glass instead of fused silica and with a path length of 5 mm instead of 10 mm. Secondly, the measurements were repeated using a different number of independently fabricated PPXC films with a lower thickness of 219 µm. Finally, the measurements were repeated using an integrating sphere detector to provide a preliminary verification that the films were non scattering (see discussion). The resulting absorption coefficient spectra are plotted in Fig. 5(c). All the spectra are in good agreement with the spectrum originally obtained in liquid.

4.2.3. PPXC absorption spectrum

The accuracies of the absorption measurements made in liquid and air were found to be wavelength dependent. The liquid measurements provided high accuracy over most of the spectral range but there were certain wavelength ranges in which the accuracy was poor due to the high absorption of the liquid. Fortunately, these wavelength ranges coincided with those in which PPXC absorption was so high that the single film measurements made in air provided acceptable accuracy. It was therefore possible to obtain an accurate absorption spectrum over almost the entire 330-3300 nm range by combining the measurements made using both methods. The measurements were combined in three steps. Firstly, all the absorption values were taken from the spectrum obtained using four films in liquid (Fig. 4). Secondly, the values were replaced by those obtained using a narrower cuvette (Fig. 5) where this provided a reduced uncertainty. This occurred when the liquid absorption coefficient was high enough to limit the accuracy in 10 mm cuvettes, but not

Optical Materials EXPRESS

so high as to prevent accurate measurements using the 5 mm cuvette. Thirdly, the values were replaced with those obtained using films in air (Fig. 4) where this provided a reduced uncertainty. This occurred in spectral regions where the liquid absorption was so high as to prevent accurate measurements being made through either cuvette. The resulting spectrum is plotted in Fig. 6.

The spectrum shows the PPXC absorption coefficient over the wavelength range 330-3300 nm. At 330 nm, the absorption coefficient is 4.3 mm^{-1}. This decreases smoothly with increasing wavelength, by about 2 orders of magnitude to about 0.05 mm^{-1} at 860 nm. Between 860 nm and 1562 nm, the absorption coefficient decreases gradually except for peaks near to 1170 nm and 1410 nm. At 1562 nm, the coefficient reaches a minimum value of 0.025 mm^{-1}. Above 1562 nm, the coefficient increases sharply to about 0.4 mm^{-1} at 1680 nm. At 1800-2100 nm, the coefficient flattens at about 0.12 mm^{-1}. At 2170-2700 nm, there are a number of peaks with maximal values in the range 0.8-1.8 mm^{-1}. At 2750-3000 nm, the coefficient flattens again at about 0.4 mm^{-1}. The coefficient then increases relatively steadily to 7.7 mm^{-1} at 3262 nm. At longer wavelengths, the coefficient was unmeasurable in our experiments because the light intensity transmitted through the sample was too low, even for a single film in air.

5. Discussion

The visible and near infrared absorption coefficient spectrum of PPXC was obtained by measuring the transmittance of single PPXC films in air and multiple films in liquid. The measured absorption coefficients ranged from 0.025 mm^{-1} to 7.7 mm^{-1} (Fig. 6), equivalent to intensity transmission losses in the range 1-350 dB/cm. For context, at wavelengths ≤850 nm, the measured absorption coefficient is at least an order of magnitude higher than that of PMMA [23]. At other wavelengths, near 1500 nm for example, the absorption coefficient is similar to that of PMMA [23]. The mean estimated uncertainty on the PPXC absorption coefficient was ±16%. Repeat measurements made using different film thicknesses, different numbers of films, different cuvettes, and different detectors yielded values in mutual agreement, suggesting the measurements were accurate.

The measurements are broadly consistent with the limited PPXC absorption data available in the literature. For example, the relative PPXC transmittance spectrum reported by Jeong et al. [3] (from which it is not possible to extract absorption coefficients because the film thickness is unknown) showed that the transmittance increased smoothly to a plateau with increasing wavelength in the range 330-1000 nm. This is consistent with the trends seen in the transmittance spectra measured in this study such as those in Fig. 4(a). Likewise, the absorbance spectrum recorded by Bera et al. [15] (prior to exposing PPXC films to UV light) showed a similar trend in the form of a decreasing absorbance with increasing wavelength in the range 300-500 nm. Moreover, as the film thickness was reported, absorption coefficients can be calculated from this data (e.g., 8.2 mm^{-1} at 330 nm, 3.6 mm^{-1} at 400 nm, and 1.4 mm^{-1} at 500 nm). These coefficients are 2-5 times higher than those measured in the present study (4.3 mm^{-1} at 330 nm, 0.86 mm^{-1} at 400 nm, and 0.28 mm^{-1} at 500 nm). However, this may be because Fresnel reflections were not accounted for by Bera et al. [15]. To test this hypothesis, we converted their absorbance into transmittance using the film thickness, then divided out the expected losses due to Fresnel reflections assuming two PPXC-air interfaces. After this correction, the calculated coefficients agreed with those measured in the present study within 0-15% at wavelengths below 395 nm. With increasing wavelength, they tended towards zero, leading to decreasing agreement. However, this could be attributed to the decreasing accuracy with increasing wavelength expected in the literature measurements due to the low PPXC film thickness (46 µm), coupled with the fact PPXC becomes increasingly transparent in this wavelength range. Of the studies reporting losses measured at single wavelengths, Xie et al. [8] reported an absorption coefficient of 0.17 mm^{-1} using a ≈470 nm LED source. This is about two times smaller than the value measured in this study (0.37 mm^{-1}) at 470 nm. Reddy et al. [6] reported waveguides losses equivalent to

Optical Materials EXPRESS

absorption coefficients of 0.14 mm^{-1} at 450 nm, 0.11 mm^{-1} at 532 nm, 0.09 mm^{-1} at 633 nm, 0.08 mm^{-1} at 680 nm. These values are 2-3 times lower than ours at 450 and 532 nm but in agreement at 633 nm and 680 nm. Overall, the fact that previously published relative spectra are broadly consistent with the measurements made here, and the few absolute absorption coefficients reported at specific wavelengths agree, at worst, within a factor of 2-3, is encouraging given the limitations of the previous studies.

In this study, measurements were made using a total of fifteen different films, drawn from two independently fabricated master films of thickness 473 µm and 219 µm. Because only two sets of independently fabricated films were used, it was not possible to rigorously investigate the impact of variability between PPXC fabrication runs, or differences in absorption that might be caused by changing the fabrication protocol. A good agreement was found, however, between the measurements obtained using the two sets of independently fabricated films. Repeat measurements made over a time period of about 18 months also agreed. The measurements therefore accurately represent PPXC films made on at least two separate occasions, films of at least two thicknesses, and films before and after lab storage over a period of up to 18 months. Although the measurements involving these films were consistent, certain fabrication parameters and environmental factors are known to affect PPXC properties including the visual appearance of films. For example, the sublimation temperature affects the film crystallinity [24] and UV light can induce yellowing [15,25], which is reflected in a change in absorbance [15]. Further studies could investigate the impact of deposition parameters, UV exposure, inter-lab variability, or other factors by applying the presented method to measure the absorption coefficient of a larger variety of PPXC films fabricated and stored differently.

To calculate PPXC absorption coefficients from the measurements made in liquid, certain assumptions were made. One assumption was that the optical thickness of the PPXC film was not changed due to the immersion of the film in the liquid. In fact, although PPXC is commonly considered an excellent chemical barrier, it has been observed to swell in certain liquids [26,27]. For films of comparable thickness to ours, the swelling has been reported as up to a few percent after tens of hours of immersion [26]. To our knowledge, this effect has not been studied in the liquid used in this study. However, even if we assume similar swelling in this liquid, as the samples were immersed for a much shorter time, any associated thickness errors would be expected to be significantly lower than a few percent. This would propagate to a negligibly small error on the absorption coefficient, suggesting this effect could be safely neglected. A second assumption involved the Cauchy equations used to provide the refractive indices of PPXC and the liquid (Fig. 2). These were known to be valid at certain wavelengths, namely 400-1000 nm for PPXC and 225-1550 nm for the liquid. However, they were also assumed to be valid at other wavelengths, at which the indices were unknown. At wavelengths below 2200 nm, there is evidence that the assumption was accurate in that the absorption measurements made in air and in liquid agreed (Fig. 5). At longer wavelengths however, the validity remains uncertain. At these wavelengths, the validity of the liquid index is unimportant because the measurements in liquid were unsuccessful due to the high liquid absorption at these wavelengths. However, any inaccuracies in the PPXC index at these wavelengths would lead to errors in the reflection corrections and subsequently in the calculated PPXC absorption coefficient. As such, the PPXC absorption coefficients measured at wavelengths <2200 nm should be treated with greater confidence than those measured at longer wavelengths.

A final question is whether the measured spectrum represents PPXC absorption only, or if it might also include losses due to scattering inside the material. Throughout this manuscript, it was assumed that absorption is the dominant process and internal scattering is negligible. Consistent with this assumption, the measurements made using an integrating sphere to capture light scattered by the sample agreed with the original measurements in which only unscattered light was detected (Fig. 5). Although this might suggest scattering was negligible, the sample was

Optical Materials EXPRESS

positioned approximately 30 cm from the sphere, rather than immediately next to it. As such, the solid angle subtended by the sphere was small and the sphere may therefore not have been able to capture enough of any scattered light to firmly conclude that there was no internal scattering. The presence of scattering could be studied more comprehensively by adapting the apparatus to place the sample immediately next to the sphere to capture more of any scattered light.

6. Conclusions

The visible and near infrared absorption coefficient spectrum of PPXC was measured using a combination of conventional PPXC film transmittance measurements and a method involving immersing multiple films in a liquid to increase sensitivity. The coefficient was found to be in the range 0.025 mm^{-1} to 7.7 mm^{-1}, equivalent to transmission losses of about 1-350 dB/cm, in the wavelength range 330-3262 nm. Confidence in the accuracy of these measurements is underscored by the consistency in the data acquired under different conditions and from multiple independent repeat experiments. In addition, where the measurements can be compared to the few limited studies in the literature, they are broadly consistent.

The PPXC absorption coefficient spectrum could be useful when designing PPXC based optical devices such as sensors and waveguides. For instance, when designing PPXC-based optical ultrasound sensors for photoacoustic imaging [9], the absorption coefficients could be included in optical models of the sensors, allowing a more accurate calculation of the expected sensor sensitivity [28]. This could aid the design of new sensors by enabling the selection of parameters such as optimal mirror reflectivities and spacer thicknesses that minimise the deleterious impact of PPXC absorption. Accurate knowledge of the PPXC absorption coefficient could also be helpful when designing PPXC waveguides to be used for optogenetics [5,8]. At wavelengths in the range 470-532 nm [5,8] for example, the measured absorption coefficient indicates a maximum $1/e$ transmission length of 3-5 mm in PPXC. This, and similar calculations, could provide an indication of the maximum permissible length for a PPXC waveguide required to deliver a given light intensity in order to elicit neuronal activation.

Beyond PPXC, the method of immersing multiple films in liquid provides a new way to measure the absorption coefficient of low-loss materials. The fundamental advantage is this provides increased sensitivity without requiring a physically thicker sample. The method also limits errors related to surface scattering and Fresnel reflections. Having described the theoretical basis and demonstrated the feasibility of this method, it could now be used to study the attenuance of other materials, especially other low-loss materials for which it is equally difficult to obtain thick samples. For example, the method could be applied to study other polymers in the Parylene family [1] such as fluorinated variants which might afford lower absorption [29–31]. Quantifying lower absorption coefficients in such materials could lead to the development of thin film optical devices with enhanced performance such as more sensitive optical ultrasound sensors and more efficient waveguides.

Funding. Royal Society (URF\R1\180435); European Research Council (741149); Engineering and Physical Sciences Research Council (EP/L016478/1); Engineering and Physical Sciences Research Council (NS/A000050/1).

Acknowledgments. The authors acknowledge Christian Sol for useful conversations concerning the refractive index of Parylene C and ellipsometry measurements.

Disclosures. The authors do not declare any financial interests or conflicts of interest.

Data availability. The PPXC absorption spectrum in Fig. 6 is available online in Dataset 1 [22]. Other data are not publicly available at this time but may be obtained from the authors upon reasonable request.

References

1. W. F. Beach, "Xylylene polymers," Encyclopedia of Polymer Science and Technology **12**, 587–626 (2002).
2. B. J. Kim and E. Meng, "Micromachining of Parylene C for bioMEMS," Polym. Adv. Technol. **27**(5), 564–576 (2016).

Optical Materials EXPRESS

3. Y. S. Jeong, B. Ratier, A. Moliton, and L. Guyard, "UV-visible and infrared characterization of poly(p-xylylene) films for waveguide applications and OLED encapsulation," Synth. Met. **127**(1-3), 189–193 (2002).
4. S. Yamagiwa, M. Ishida, T. Kawano, S. Yamagiwa, M. Ishida, and T. Kawano, "Flexible parylene-film optical waveguide arrays," Appl. Phys. Lett. **083502**(2015), 1–6 (2016).
5. J. W. Reddy and M. Chamanzar, "Low-loss flexible Parylene photonic waveguides for optical implants," Opt. Lett. **43**(17), 4112 (2018).
6. J. W. Reddy, M. Lassiter, and M. Chamanzar, "Parylene photonics: a flexible, broadband optical waveguide platform with integrated micromirrors for biointerfaces," Microsyst Nanoeng **6**(1), 85 (2020).
7. O. I. Szentesi and E. A. Noga, "Parylene C films for optical waveguides," Appl. Opt. **13**(11), 2458–2459 (1974).
8. T. Xie, X. Bi, R. Luo, F. Bin, Z. Wang, and W. Li, "Optical propagation of blue LED light in brain tissue and Parylene-C," *2017 IEEE 12th Int. Conf. Nano/Micro Eng. Mol. Syst. NEMS 2017*, vol. 2 (2017), 599–602.
9. E. Zhang, J. Laufer, and P. Beard, "Backward-mode multiwavelength photoacoustic scanner using a planar Fabry-Perot polymer film ultrasound sensor for high-resolution three-dimensional imaging of biological tissues," Appl. Opt. **47**(4), 561–577 (2008).
10. J. Buchmann, J.A. Guggenheim, E. Z. Zhang, C. Scharfenorth, B. Spannekrebs, C. Villringer, and J. Laufer, "Characterization and modeling of Fabry–Perot ultrasound sensors with hard dielectric mirrors for photoacoustic imaging," Appl. Opt. **56**(17), 5039 (2017).
11. P. Hajireza, K. Krause, M. Brett, and R. Zemp, "Glancing angle deposited nanostructured film Fabry-Perot etalons for optical detection of ultrasound," Opt. Express **21**(5), 6391 (2013).
12. P. Morris, A. Hurrell, A. Shaw, E. Zhang, and P. Beard, "A Fabry-Perot fiber-optic ultrasonic hydrophone for the simultaneous measurement of temperature and acoustic pressure," J. Acoust. Soc. Am. **125**(6), 3611–3622 (2009).
13. S. Dufour and Y. De Koninck, "Optrodes for combined optogenetics and electrophysiology in live animals," Neurophotonics **2**(3), 031205 (2015).
14. J. A. Guggenheim, J. Li, T. J. Allen, R. J. Colchester, S. Noimark, O. O. Ogunlade, I. P. Parkin, I. Papakonstantinou, A. E. Desjardins, E. Z. Zhang, and P. C. Beard, "Ultrasensitive plano-concave optical microresonators for ultrasound sensing," Nat. Photonics **11**(11), 714–719 (2017).
15. M. Bera, A. Rivaton, C. Gandon, and J. L. Gardette, "Comparison of the photodegradation of parylene C and parylene N," Eur. Polym. J. **36**(9), 1765–1777 (2000).
16. G. Gauglitz and T. Vo-Dinh, *Handbook of Spectroscopy* Wiley-VCH Verlag GmbH & Co. KGaA, Weinheim, FRG (2003).
17. A. Hordvik, "Measurement techniques for small absorption coefficients: recent advances," Appl. Opt. **16**(11), 2827 (1977).
18. A. V. Khomchenko, "Waveguide spectroscopy of thin films," Tech. Phys. Lett. **27**(4), 271–274 (2001).
19. W. Heitmann, "Attenuation measurement in glasses for optical communications: an immersion method," Appl. Opt. **15**(1), 256 (1976).
20. J. F. Gaynor and S. B. Desu, "Optical properties of polymeric thin films grown by chemical vapor deposition," J. Mater. Res. **11**(1), 236–242 (1996).
21. G. M. Hale and M. R. Querry, "Optical Constants of Water in the 200-nm to 200-Mm Wavelength Region," Appl. Opt. **12**(3), 555–563 (1973).
22. J. A. Guggenheim, Y. Lyu, D. M. Marques, E. Z. Zhang, and P. C. Beard, "Parylene C absorption coefficient spectrum," figshare, (2021). https://doi.org/10.6084/m9.figshare.14564550.
23. R. C. Progelhof, J. Franey, and T. W. Haas, "Absorption coefficient of unpigmented poly(methyl methacrylate), polystyrene, polycarbonate, and poly(4-methylpentene-1) sheets," J. Appl. Pol **15**(7) 1803–1807 (1971).
24. G. Surendran, M. Gazicki, W. J. James, and H. Yasuda, "Polymerization of para-xylylene derivatives. V. Effects of the sublimation rate of di-p-xylylene on the crystallinity of parylene C deposited at different temperatures," J. Polym. Sci. Part A Polym. Chem. **25**(8), 2089–2106 (1987).
25. G. Maggioni, A. Tessarollo, and S. Carturan, "Study of the effects of incorporation of UV-absorbing compound in parylene C films," Mater. Chem. Phys. **149**, 530–538 (2015).
26. E. Miller and E. Leighton, "Swelling of Parylene C," J. Elastomers Plast. **22**(1), 46–57 (1990).
27. H. C. Koydemir, H. Külah, and C. Özgen, "Solvent compatibility of parylene c film Layer," J. Microelectromech. Syst. **23**(2), 298–307 (2014).
28. D. M. Marques, J. A. Guggenheim, R. Ansari, E. Z. Zhang, P. C. Beard, and P. R. T. Munro, "Modelling Fabry-Pérot etalons illuminated by focussed beams," Opt. Express **28**(5), 7691 (2020).
29. A. Kahouli, A. Sylvestre, J. F. Laithier, L. Lutsen, S. Pairis, E. André, and J. L. Garden, "Structural and dielectric properties of parylene-VT4 thin films," Mater. Chem. Phys. **143**(3), 908–914 (2014).
30. A. Kahouli, A. Sylvestre, F. Jomni, E. André, J. L. Garden, B. Yangui, B. Berge, and J. Legrand, "Dielectric properties of parylene AF4 as low-k material for microelectronic applications," Thin Solid Films **520**(7), 2493–2497 (2012).
31. W. R. Dolbier and W. F. Beach, "Parylene-AF4: A polymer with exceptional dielectric and thermal properties," Journal of Fluorine Chemistry **122**(1), 97–104 (2003).